

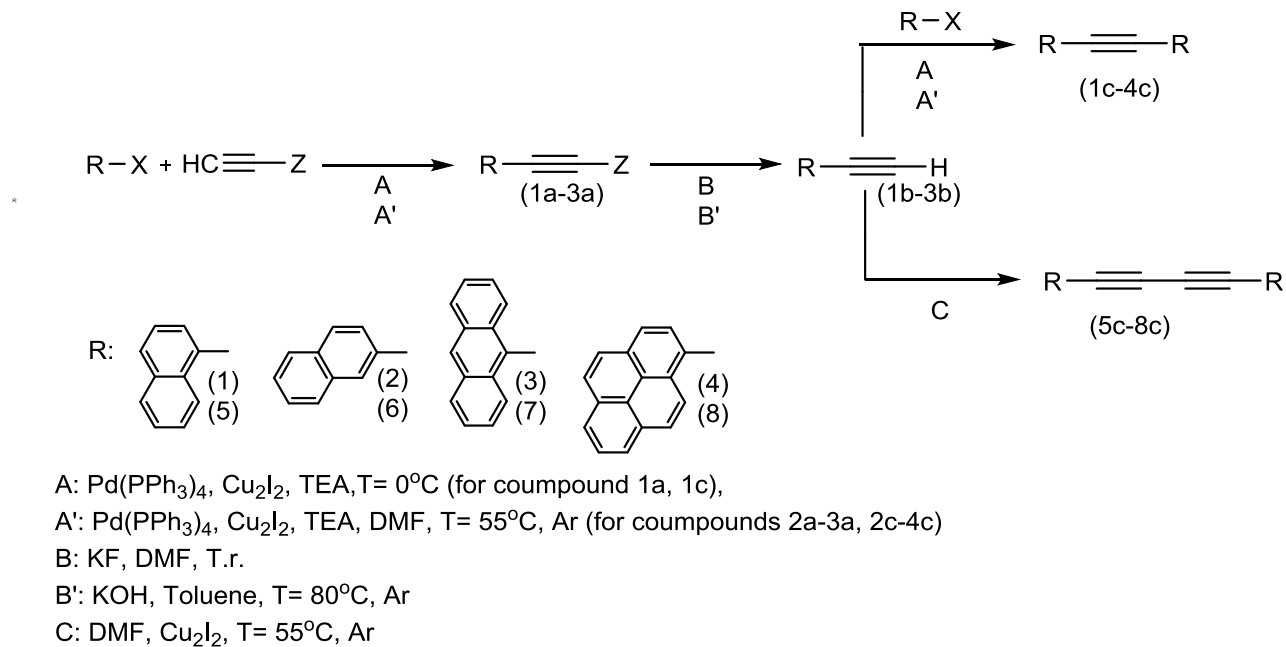
Electronic Supporting Informations

Photophysical properties of the symmetrically substituted
diarylacetlenes and diarylbuta-1,3-diynes.

Irena Bylińska, Małgorzata Wierzbicka, Cezary Czaplewski,
Wiesław Wiczk*

Faculty of Chemistry, University of Gdańsk
80-308 Gdańsk, Wita Stwosza 63, Poland

Scheme 1. Synthesis of 1c-4c monoacetylene and 5c-8c buta-1,3-diyne derivatives.



Compound	-X	-Z
(1)	-I	-TMS
(2)	-Br	-C(CH ₃) ₂ (OH)
(3)		-
(4)		-

Identification data for all compounds studied.

1,2-di(naphthalen-1-yl)ethyne (1c) (yield 40.2%)

¹H-NMR (500 MHz, CDCl₃):

δ_{H} (ppm): 7.58 (t, 2H, C¹⁰H, C^{10'}H); 7.60 (t, 2H, C⁶H, C^{6'}H); 7.64 (t, 2H, C⁵H, C^{5'}H); 7.90 (m, 6H, C⁷H, C^{7'}H, C⁹H, C^{9'}H, C¹¹H, C^{11'}H); 8.57 (d, 2H, C⁴H, C^{4'}H);

¹³C-NMR (100 MHz, CDCl₃)

δ_{C} (ppm): 78.29 C¹, C^{1'}; 121.1 C², C^{2'}; 125.73 C⁶, C^{6'}; 126.44 C¹⁰, C^{10'}; 126.65 C⁴, C^{4'}; 127.1 C⁵, C^{5'}; 128.51 C⁷, C^{7'}; 129.0 C⁹, C^{9'}; 130.75 C¹¹, C^{11'}; 133.00 C³, C^{3'}; 133.27 C⁸, C^{8'};

MS (m/z): 279 (M+H)⁺;

Ramman $\nu_{\text{max}}(\text{cm}^{-1})$: 2203.4 C≡C;

1,2-di(naphthalen-2-yl)ethyne (2c) (yield 32.6%)

¹H-NMR (500 MHz, CDCl₃):

δ(ppm): 7.51 - 7.54 (m, 4H, C⁶H, C^{6'}H, C⁷H, C^{7'}H); 7.55 (d, 2H, C¹¹H, C^{11'}H); 7.80-8.84 (m, 6H, C⁵, C^{5'}, C⁸, C^{8'}C¹⁰H, C^{10'}H,); 8.09 (s, 2H, C³H, C^{3'}H);

¹³C-NMR (100 MHz, CDCl₃)

δ_C (ppm): 82.44 C¹, C^{1'}; 119.31 C², C^{2'}; 126.99 C⁶, C^{6'}; 127.49 C¹⁰, C^{10'}; 128.04 C⁸, C^{8'}; 128.08 C⁵, C^{5'}; 128.40 C⁷, C^{7'}; 128.71 C¹¹, C^{11'}; 133.07 C⁴, C^{4'}; 133.26 C³, C^{3'}; 133.43 C⁹, C^{9'};

MS (m/z) : 279 (M+H)⁺;

Ramman ν_{max}(cm⁻¹): 2219.6 C≡C;

1,2-di(anthracen-9-yl)ethyne (3c) (yield 33.3%)

¹H-NMR (500 MHz, CDCl₃):

δ(ppm): 7.50-7.61 (m, 4H, C⁶H, C^{6'}H, C¹²H, C^{12'}H); 7.62-7.78 (m, 4H, C⁵H, C^{5'}H, C¹³H, C^{13'}H); 8.1 (d, 4H, C⁷H, C^{7'}H C¹¹H, C^{11'}H); 8.54 (s, 2H, C⁹, C^{9'}); 8.64-8.66 (m, 4H, C⁴H, C^{4'}H, C¹⁴H, C^{14'}H);

¹³C-NMR (100 MHz, CDCl₃)

δ(ppm): 82.12 C¹, C^{1'}; 120.15 C³, C^{3'}; 122.43 C⁶, C^{6'}, C¹², C^{12'}; 125.75 C⁵, C^{5'}, C¹³, C^{13'}; 126.91 C⁴, C^{4'}, C¹⁴, C^{14'}; 126.99 C⁹, C^{9'}; 128.41 C⁷, C¹¹, C^{7'}, C^{11'}; 130.00 C⁸, C^{8'}, C¹⁰, C^{10'}; 133.70 C³, C^{3'}, C¹⁵, C^{15'};

MS (m/z): 379 [M+H]⁺;

Ramman ν_{max}(cm⁻¹): 2183.8 C≡C;

1,2-di(pyren-1-yl)ethyne (4c) (yield 8.0%)

¹H-NMR (500 MHz, CDCl₃): 7.94-8.04 (t, 2H, C⁸H, C^{8'}H); 8.05-8.12 (m, 4H, C¹¹H, C^{11'}H, C¹², C^{12'}); 8.17 (m, 4H, C⁵, C^{5'}, C¹⁵H, C^{15'}H); 8.20-8.23 (m, 4H, C⁴H, C^{4'}H, C¹⁴H, C^{14'}H); 8.34 (d, 2H, C⁹H, C^{9'}H), 8.44 (d, 2H, C⁷H, C^{7'}H);

¹³C-NMR (100 MHz, CDCl₃):

δ(ppm): 81.12 C¹, C^{1'}; 110.15 C¹⁷, C^{17'}; 112.45 C¹², C^{12'}; 115.31 C¹⁵, C^{15'}; 116.01 C⁴, C^{4'}; 117.10 C⁹, C^{9'}; 118.22 C⁸, C^{8'}; 124.63 C⁷, C^{7'}; 125.73 C¹⁶, C^{16'}; 126.41 C⁵, C^{5'}; 127.30 C¹¹, C^{11'}; 128.17 C³, C^{3'}; 128.61 C², C^{2'}; 129.97 C¹³, C^{13'}; 131.36 C¹⁰, C^{10'}; 131.41 C⁶, C^{6'}; 132.02 C¹⁴, C^{14'};

MS (m/z): 426 [M]

Ramman ν_{max}(cm⁻¹): 2187 C≡C;

1,4-di(naphthalen-1-yl)buta-1,3-diyne (5c) (yield 34.2%)

¹H-NMR (500 MHz, CDCl₃):

δ (ppm): 7.44-7.5 (m, 2H, C₁₁H, C_{11'}H); 7.52-7.58 (m, 2H, C₇H, C_{7'}H); 7.62-7.66 (m, 2H, C₆H, C_{6'}H); 7.82-7.86 (m, 2H, C₁₂H, C_{12'}H); 7.88-7.92 (dd, 4H, C₈H, C_{8'}H, C₁₀H, C_{10'}H, J=2 Hz, J=4 Hz); 8.42-8.46 (d, 2H, C₅H, C_{5'}H, J=4 Hz);
¹³C-NMR: 74.59 C¹, C^{1'}; 82.41 C², C^{2'}; 119.30 C³, C^{3'}; 127.00 C⁷, C^{7'}; 127.35 C¹¹, C^{11'}; 128.09 C⁹, C^{9'}; 128.17 C⁶, C^{6'}; 128.48 C⁸, C^{8'}; 128.71 C¹², C^{12'}; 133.18 C⁵, C^{5'}; 133.27 C⁴, C^{4'}; 133.47 C¹⁰, C^{10'};

MS (m/z): 302 (M);

Ramman ν_{max}(cm⁻¹): 2205.4 C≡C;

1,4-di(naphthalen-2-yl)buta-1,3-diyne (6c) (yield 35.5%)

¹H-NMR (500 MHz, CDCl₃):

δ(ppm): 7.49-7.59 (m, 6H, C⁷H, C⁸H, C¹²H, C^{7'}H, C^{8'}H, C^{12'}H); 7.78-7.86 (m, 6H, C⁶H, C⁹H, C¹¹H, C^{6'}H, C^{9'}H, C^{11'}H); 8.09 (s, 2H, C⁴H, C^{4'}H);

¹³C-NMR (100 MHz, CDCl₃)

δ(ppm): 74.61 C¹, C^{1'}; 82.44 C², C^{2'}; 119.32 C³, C^{3'}; 127.00 C⁷, C^{7'}; 127.45 C¹¹, C^{11'}; 128.05 C⁹, C^{9'}; 128.09 C⁶, C^{6'}; 128.41 C⁸, C^{8'}; 128.71 C¹², C^{12'}; 133.08 C⁵, C^{5'}; 133.27 C⁴, C^{4'}; 133.44 C¹⁰, C^{10'};

MS (m/z): 302 (M);

Ramman ν_{max}(cm⁻¹): 2215.5 C≡C;

1,4-di(anthracen-9-yl)buta-1,3-diyne (7c) (yield 43.6%)

¹H-NMR (500 MHz, CDCl₃):

δ(ppm): 7.50-7.60 (m, 4H, C⁷H, C¹³H, C^{7'}H, C^{13'}H); 7.63-7.72 (m, 4H, C⁶H, C¹⁴H, C^{6'}H, C^{14'}H); 8.52 (d, 4H, C⁸H, C¹²H, C^{8'}H, C^{12'}H); 8.50 (s, 2H, C¹⁰H, C^{10'}H); 8.71 (d, 4H, C⁵H, C¹⁵H, C^{5'}H, C^{15'}H);

¹³C-NMR (100 MHz, CDCl₃)

δ(ppm): 81.82 C¹, C^{1'}; 88.34 C², C^{2'}; 121.35 C⁷, C¹³, C^{7'}, C^{13'}; 123.50 C³, C^{3'}; 126.15 C⁶, C¹⁴, C^{6'}, C^{14'}; 126.91 C⁵, C¹⁵, C^{5'}, C^{15'}; 127.49 C¹⁰, C^{10'}; 129.12 C⁸, C¹², C^{8'}, C^{12'}; 131.38 C⁹, C¹¹, C^{9'}, C^{11'}; 134.30 C⁴, C¹⁶, C^{4'}, C^{16'};

MS (m/z): 402 (M);

Ramman ν_{max}(cm⁻¹): 2200.5 C≡C;

1,4-di(pyren-1-yl)buta-1,3-diyne (8c) (yield 30.0%)

¹H-NMR (500 MHz, DMSO): 7.50-7.70 (m, 4H, C12H, C13H, C12'H, C13'H); 7.79-7.90 (t, 2H, C9H, C9'H); 8.16-8.24 (m, C6H, C6'H); 8.26-8.34 (d, 2H, C16H, C16'H); 8.34-8.40 (m, 2H, C15H, C15'H); 8.42-8.45 (m, 2H ,C5H, C5'H); 8.46-8.50 (m, 2H, C10H, C10'H), 8.61-8.68 (d, 2H, C8H, C8'H);

¹³C-NMR (100 MHz, CDCl₃): too low solubility to collect the spectrum

MS (m/z): 451 (M+H)⁺;

Ramman $\nu_{\text{max}}(\text{cm}^{-1})$: 2195.92 C≡C.

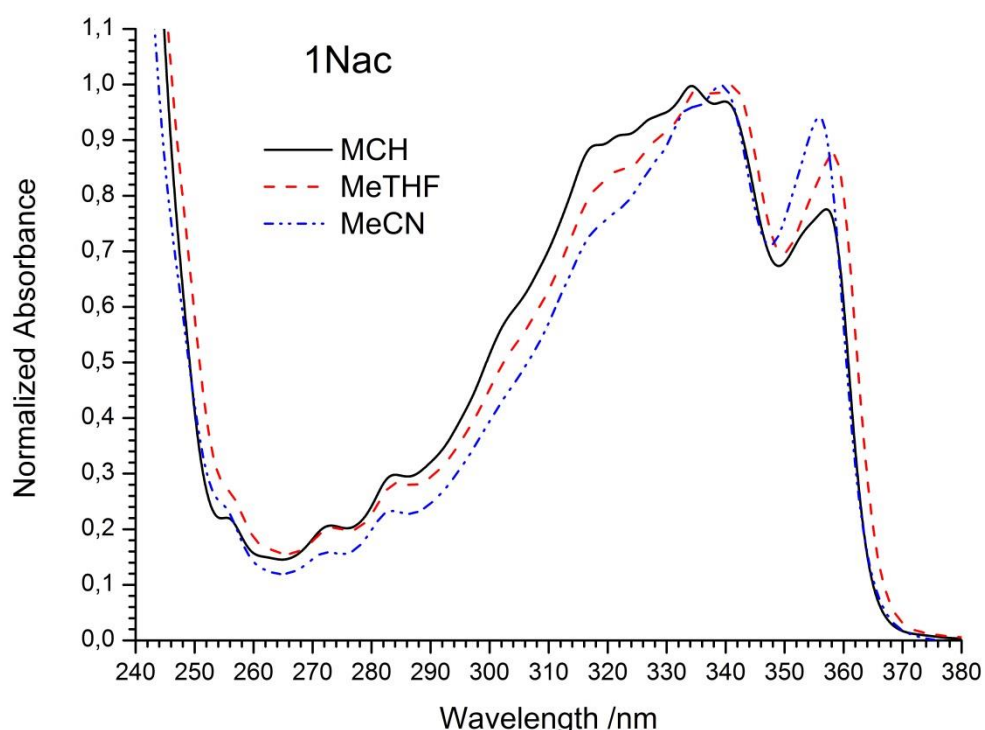


Fig. 1 ESI Absorption spectra of 1Nac in methylcyclohexane, MCH (solid dark line), 2-methyltetrahydrofuran MeTHF (dashed red line) and acetonitrile MeCN (dash-dotted blue line).

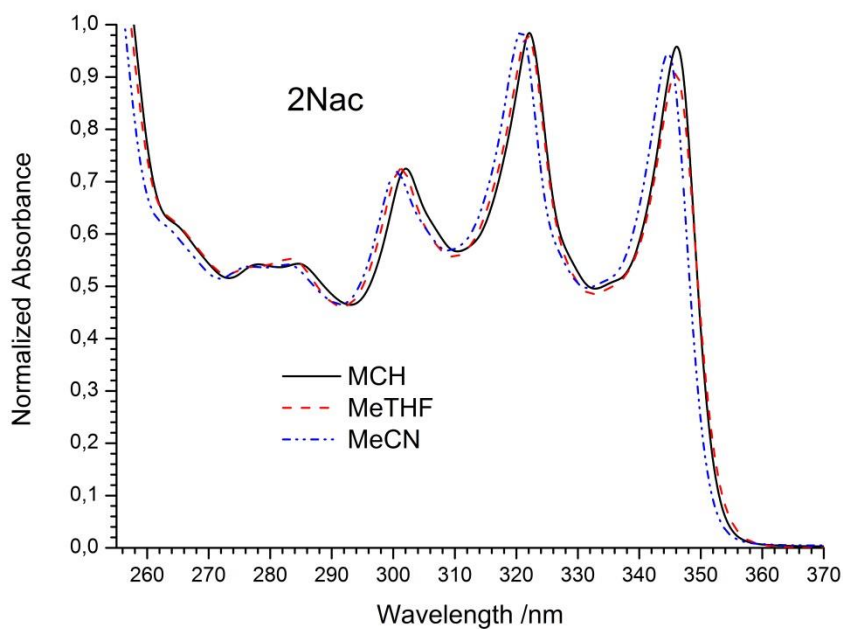


Fig. 2 ESI Absorption spectra of 2Nac in methylcyclohexane (solid dark line), 2-methyltetrahydrofuran (dashed red line) and acetonitrile (dash-dotted blue line).

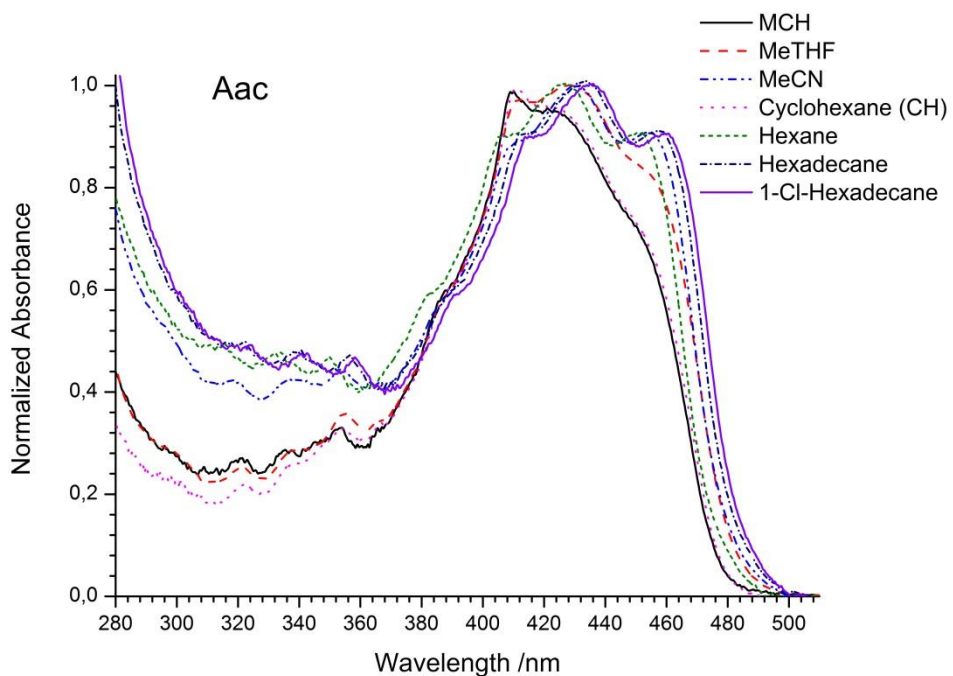


Fig. 3 ESI Absorption spectra of Aac in methylcyclohexane (solid dark line), 2-methyltetrahydrofuran (dashed red line) and acetonitrile (dash-dotted blue line), cyclohexane (dotted red line), hexane (short-dashed green line), hexadecane (dash-dot navy line), 1-chloro-hexadecane solid violet line).

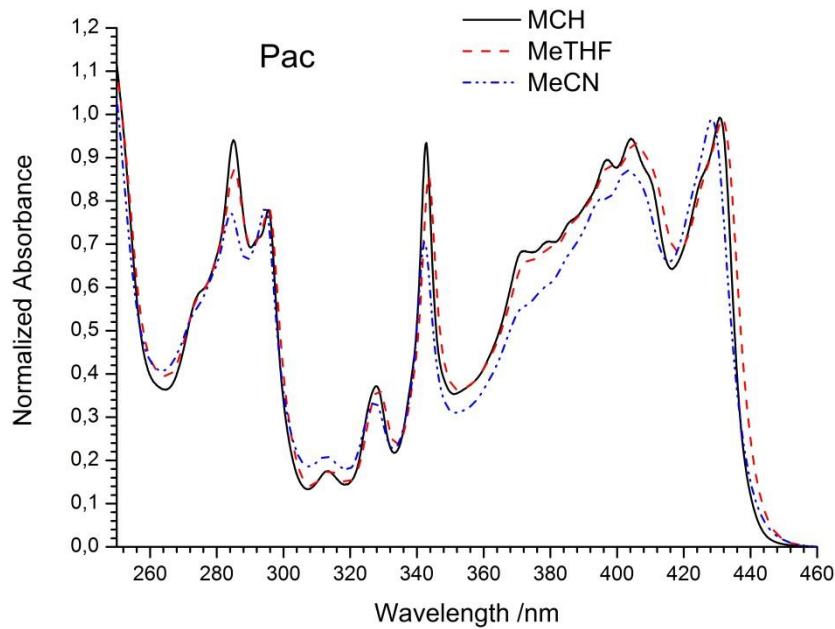


Fig. 4 ESI Absorption spectra of Pac in methylcyclohexane (solid dark line), 2-methyltetrahydrofuran (dashed red line) and acetonitrile (dash-dotted blue line).

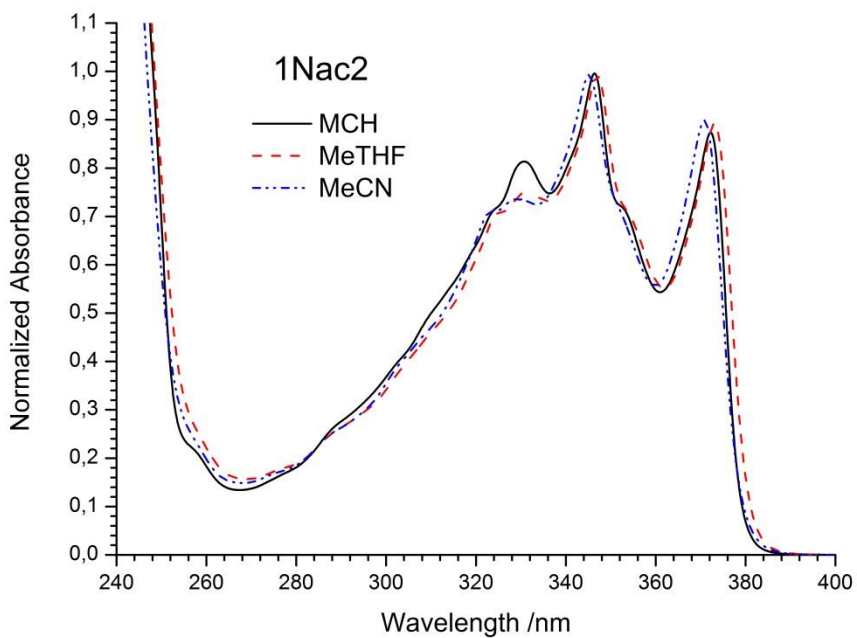


Fig. 5 ESI Absorption spectra of 1Nac2 in methylcyclohexane (solid dark line), 2-methyltetrahydrofuran (dashed red line) and acetonitrile (dash-dotted blue line).

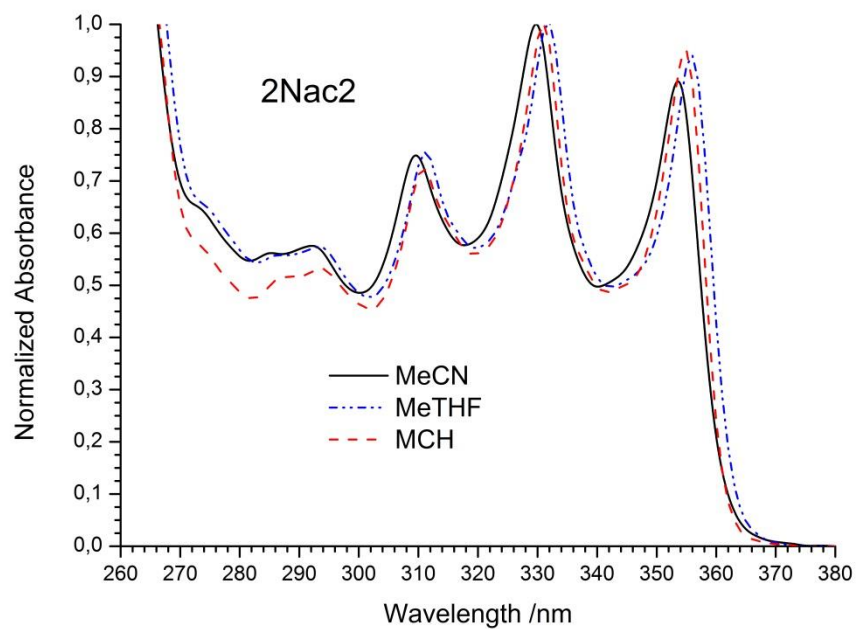


Fig. 6 ESI Absorption spectra of 2Nac2 in methylcyclohexane (solid dark line), 2-methyltetrahydrofuran (dashed red line) and acetonitrile (dash-dotted blue line).

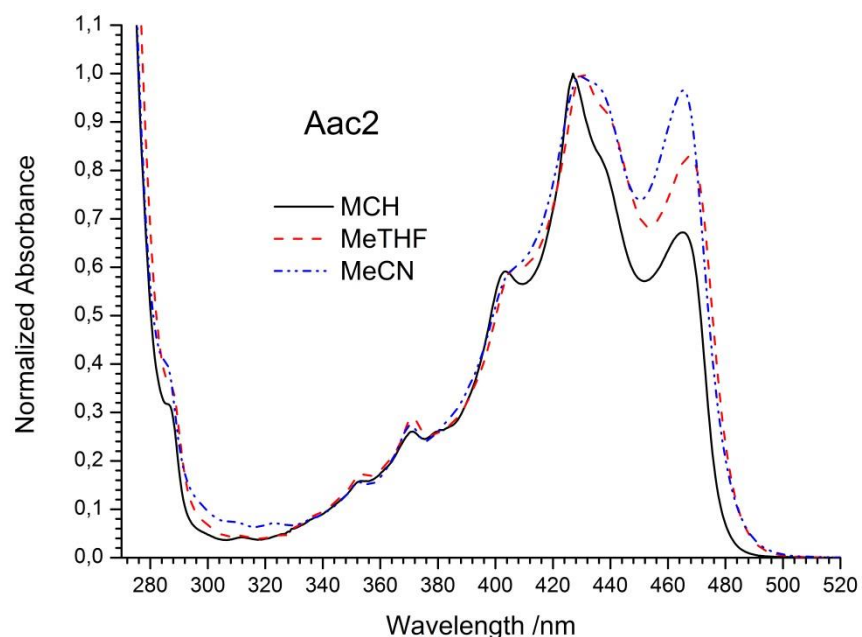


Fig. 7 ESI Absorption spectra of Aac2 in methylcyclohexane (solid dark line), 2-methyltetrahydrofuran (dashed red line) and acetonitrile (dash-dotted blue line).

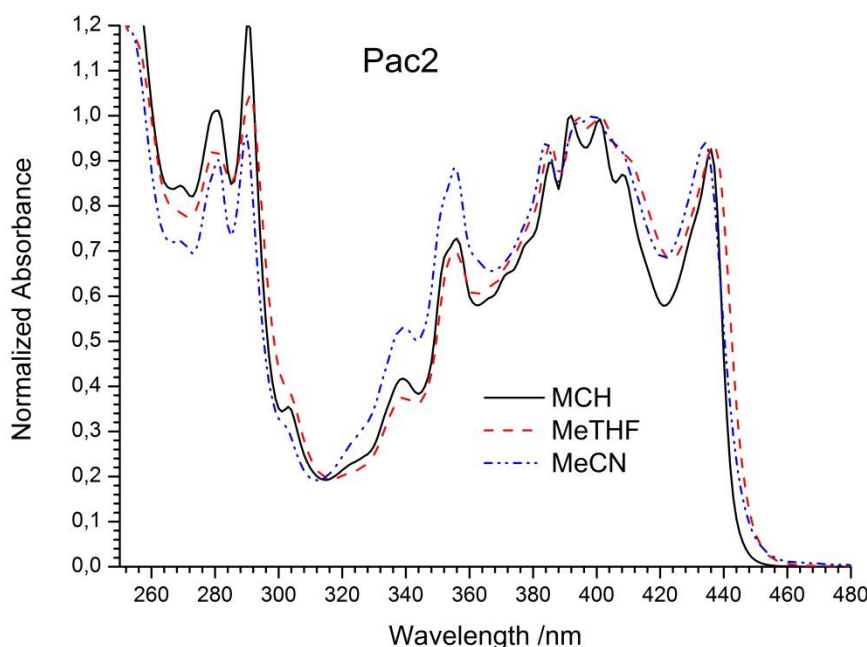


Fig. 8 ESI Absorption spectra of Pac2 in methylcyclohexane (solid dark line), 2-methyltetrahydrofuran (dashed red line) and acetonitrile (dash-dotted blue line).

Table 1 ESI Long-wave absorption and fluorescence band position of compounds studied in methyl-cyclohexane and differences in absorption and emission long-wave band between acetylene and buta-1,3-diyne derivatives.

Acetylene derivative	$\lambda_{\text{abs}} / \text{nm}$	$\lambda_{\text{fluo}} / \text{nm}$	Buta-1,3-diyne derivative	$\lambda_{\text{abs}} / \text{nm}$	$\lambda_{\text{fluo}} / \text{nm}$	$\Delta \lambda_{\text{abs}} / \text{nm}$	$\Delta \lambda_{\text{fluo}} / \text{nm}$
1Nac	357	362	1Nac2	372	376	15	14
2Nac	346	342	2Nac2	355	359	9	17
1Pac	430	434	Pac2	436	440	6	6
Aac	455	467 (shoulder)	Aac2	465	474	8	7

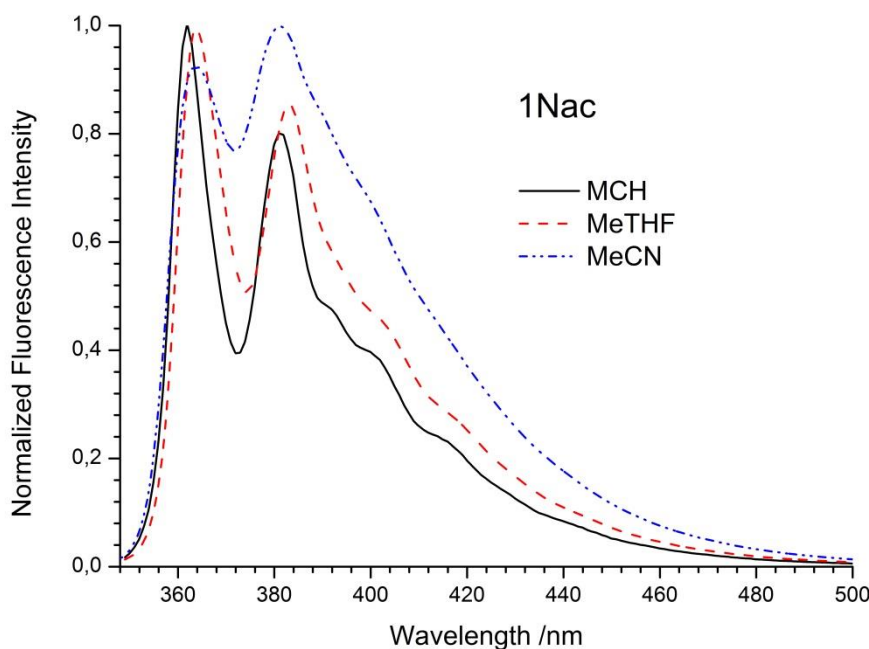


Fig. 9 ESI Emission spectra of 1Nac in methylcyclohexane (solid black line), 2-methyltetrahydrofuran (dashed red line) and acetonitrile (dash-dotted blue line).

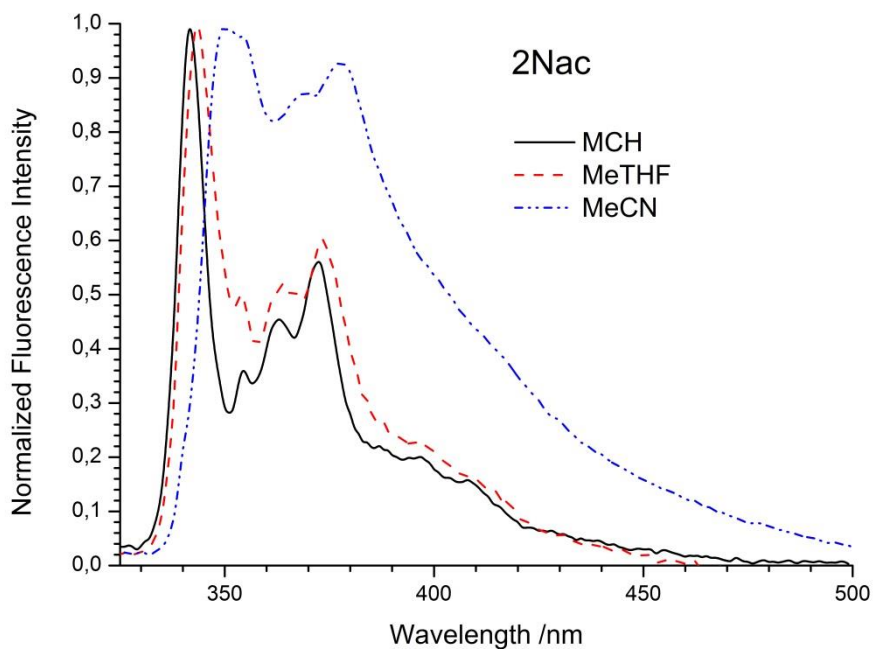


Fig. 10 ESI Emission spectra of 2Nac in methylcyclohexane (solid black line), 2-methyltetrahydrofuran (dashed red line) and acetonitrile (dash-dotted blue line).

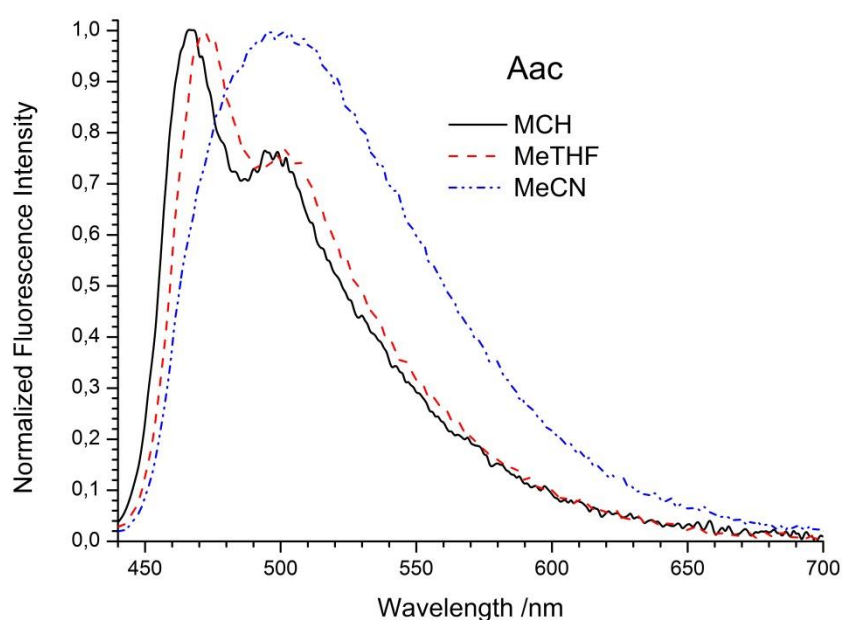


Fig. 11 ESI Emission spectra of Aac in methylcyclohexane (solid black line), 2-methyltetrahydrofuran (dashed red line) and acetonitrile (dash-dotted blue line).

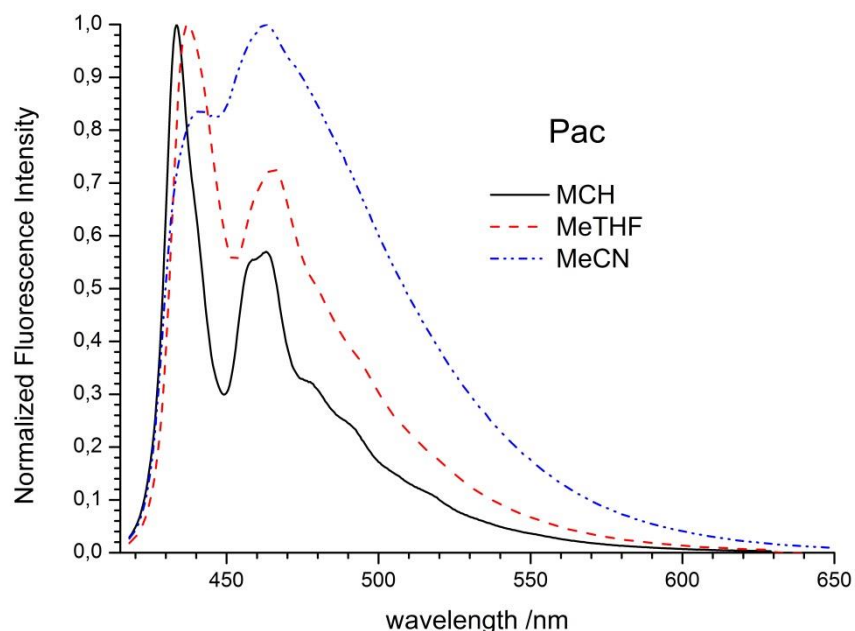


Fig. 12 ESI Emission spectra of Pac in methylcyclohexane (solid black line), 2-methyltetrahydrofuran (dashed red line) and acetonitrile (dash-dotted blue line).

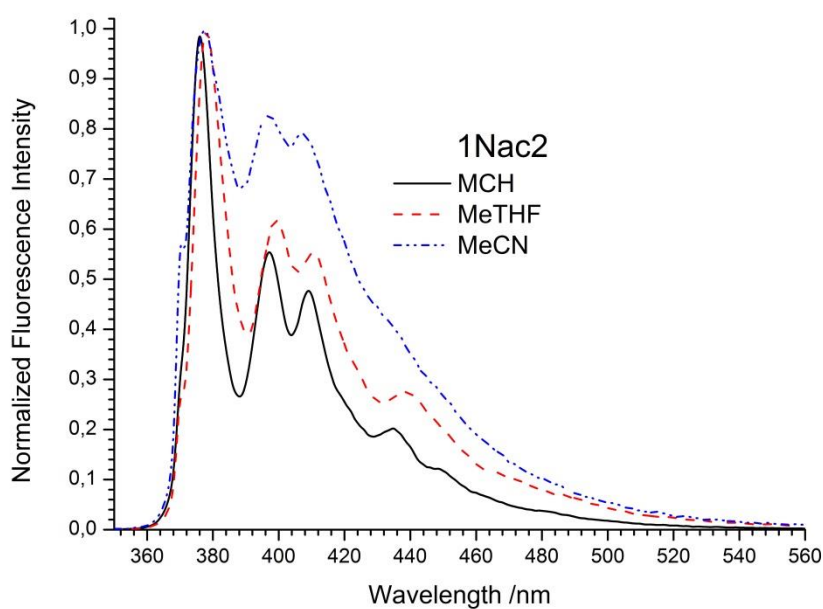


Fig. 13 ESI Emission spectra of 1Nac2 in methylcyclohexane (solid black line), 2-methyltetrahydrofuran (dashed red line) and acetonitrile (dash-dotted blue line).

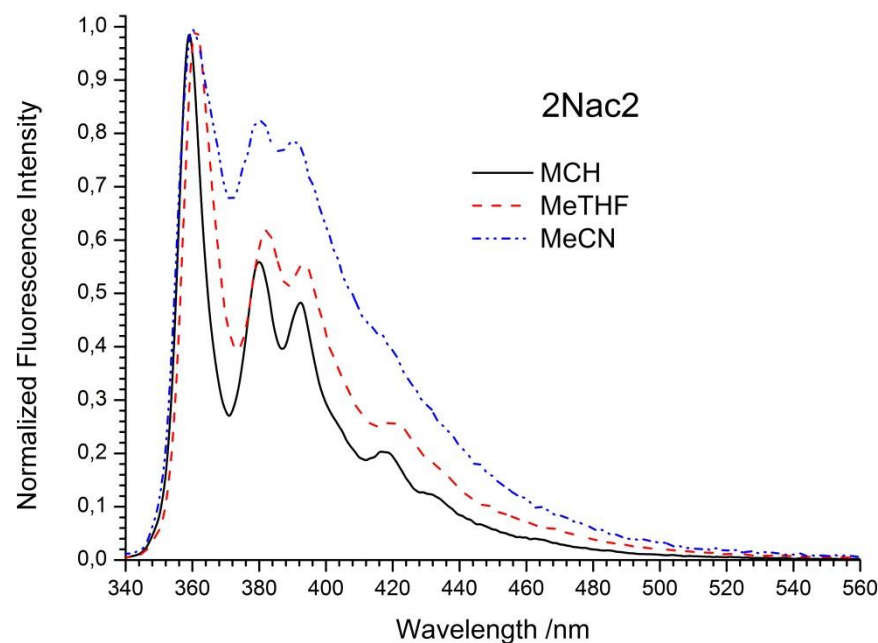


Fig. 14 ESI Emission spectra of 2Nac2 in methylcyclohexane (solid black line), 2-methyltetrahydrofuran (dashed red line) and acetonitrile (dash-dotted blue line).

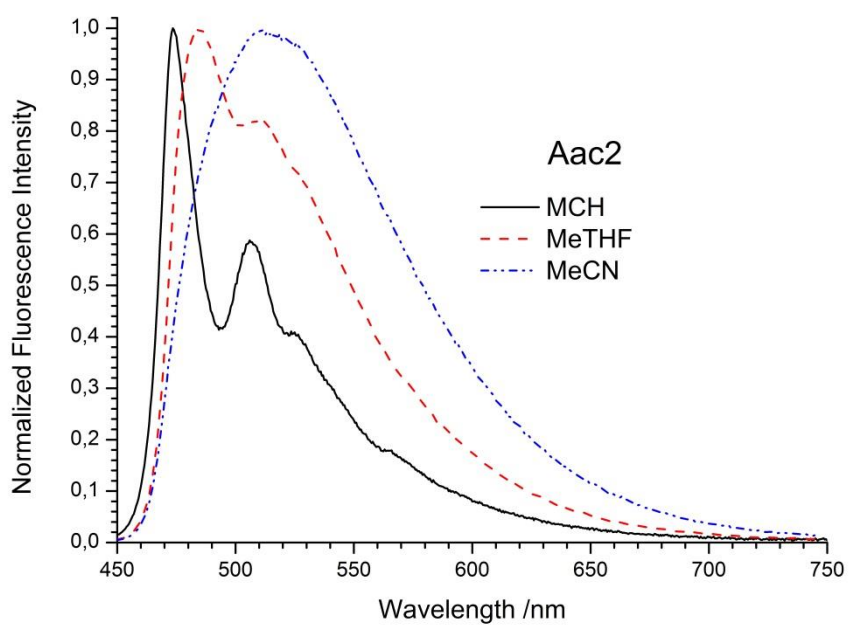


Fig. 15 ESI Emission spectra of Aac2 in methylcyclohexane (solid black line), 2-methyltetrahydrofuran (dashed red line) and acetonitrile (dash-dotted blue line).

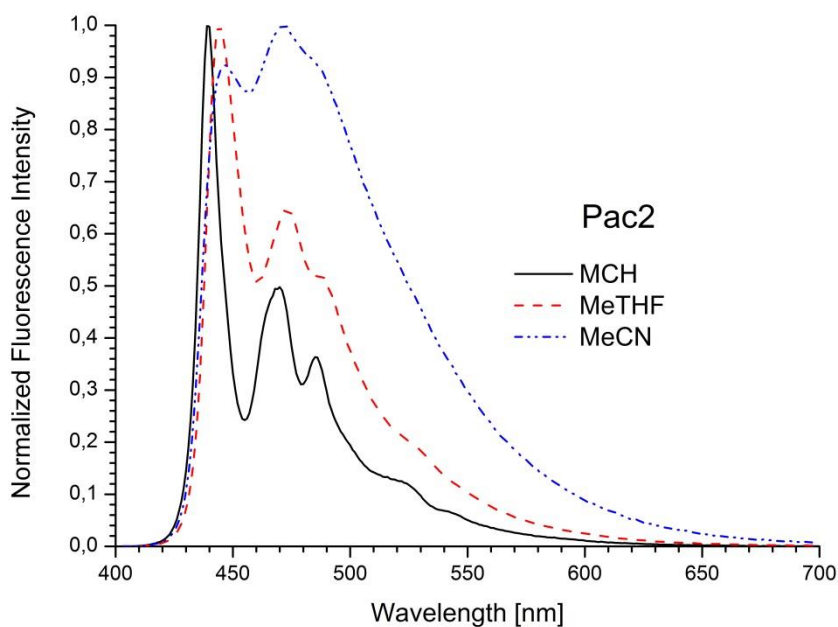


Fig. 16 ESI Emission spectra of Pac2 in methylcyclohexane (solid black line), 2-methyltetrahydrofuran (dashed red line) and acetonitrile (dash-dotted blue line).

Table 2 ESI Fluorescence quantum yield (ϕ), fluorescence lifetime (τ), pre-exponential factor (α) and quality of fit χ^2_R of studied compounds in different solvents.
 (CH-cyclohexane, C₆H₁₄-hexane, C₁₆H₃₄-hexadecane, C₁₆H₃₃Cl- 1-Cl-hexadecane, SQ –squalene)

Compound	Solvent	ϕ	τ/ns	α	χ^2_R
1Nac	CH	0.735	1.57	1	0.95
	C ₆ H ₁₄	0.758	1.46	1	0.97
	C ₁₆ H ₃₄	0.742	1.68	1	1.02
	C ₁₆ H ₃₃ Cl	0.784	1.72	1	1.05
	SQ	0.771	1.68	1	1.11
1Nac2	CH	0.161	0.29	1	1.04
	C ₆ H ₁₄	0.132	0.25	1	1.02
	C ₁₆ H ₃₄	0.173	0.29	1	1.02
	C ₁₆ H ₃₃ Cl	0.187	0.34	1	0.93
	SQ	0.181	0.35	1	0.90
2Nac	CH	0.117	0.48	1	1.04
	C ₆ H ₁₄	0.174	4.87 0.45	0.040 0.960	0.96
	C ₁₆ H ₃₄	0.208	4.44 0.62	0.124 0.876	0.95
	C ₁₆ H ₃₃ Cl	0.216	4.79 0.44	0.108 0.892	0.94
	SQ	0.224	4.81 0.43	0.105 0.985	1.12
2Nac2	CH	0.009	2.62 0.14	0.062 0.938	0.95
	C ₆ H ₁₄	0.009	2.41 0.18	0.061 0.939	0.97
	C ₁₆ H ₃₄	0.0095	2.58 0.24	0.052 0.948	1.17
	C ₁₆ H ₃₃ Cl	0.0100	2.65 0.33	0.055 0.945	0.93
	SQ	0.0106	2.61 0.29	0.060 0.940	0.86
Aac	CH	0.584	1.65	1	1.00
	C ₆ H ₁₄	0.624	1.73	1	1.01
	C ₁₆ H ₃₄	0.598	1.79 0.66	0.916 0.084	1.16
	C ₁₆ H ₃₃ Cl	0.657	2.08 0.57	0.887 0.113	0.95
	SQ	0.660	2.24 0.61	0.884 0.116	1.05
Aac2	CH	0.167	3.88 0.92	0.176 0.824	0.98
	C ₆ H ₁₄	0.161	3.57 0.81	0.126 0.874	0.94
	C ₁₆ H ₃₄	0.163	3.72 0.92	0.190 0.810	0.90
	C ₁₆ H ₃₃ Cl	0.187	4.08 1.34	0.119 0.881	0.90
	SQ	0.237	4.11 1.18	0.110 0.890	0.97
Pac	CH	0.982	1.37	1	0.97
	C ₆ H ₁₄	1.00	1.36	1	1.00
	C ₁₆ H ₃₄	0.993	1.46	1	1.02
	C ₁₆ H ₃₃ Cl	0.982	1.45	1	1.10
	SQ	0.913	1.44	1	0.96
Pac2	CH	0.793	1.16	1	0.95
	C ₆ H ₁₄	0.788	1.15	1	0.98
	C ₁₆ H ₃₄	0.793	1.21	1	1.00
	C ₁₆ H ₃₃ Cl	0.669	1.26	1	0.98
	SQ	0.659	1.19	1	0.99

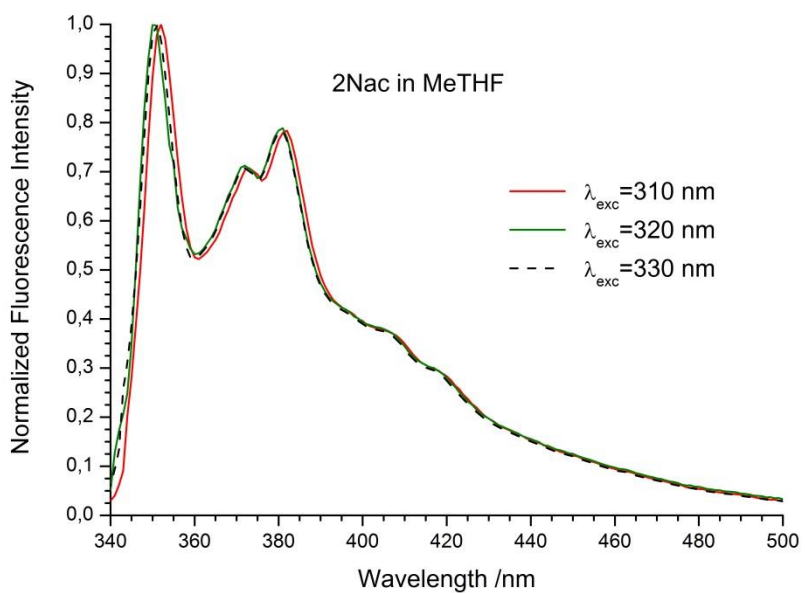


Fig. 17 ESI Emission spectra of 2Nac in 2-methyltetrahydrofuran recorded at different excitation wavelengths.

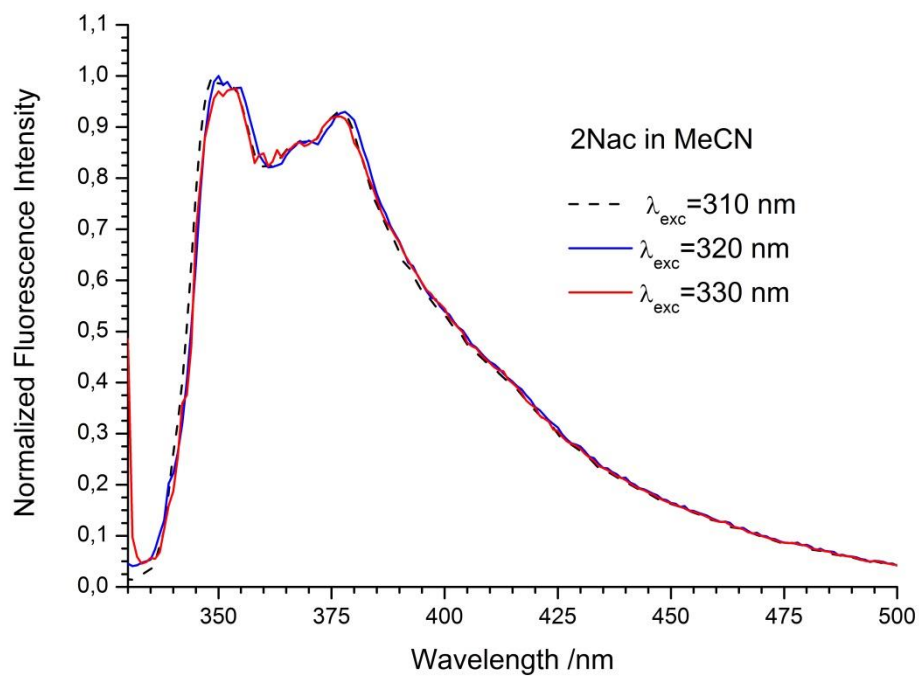


Fig. 18 ESI Emission spectra of 2Nac in acetonitrile recorded at different excitation wavelengths.

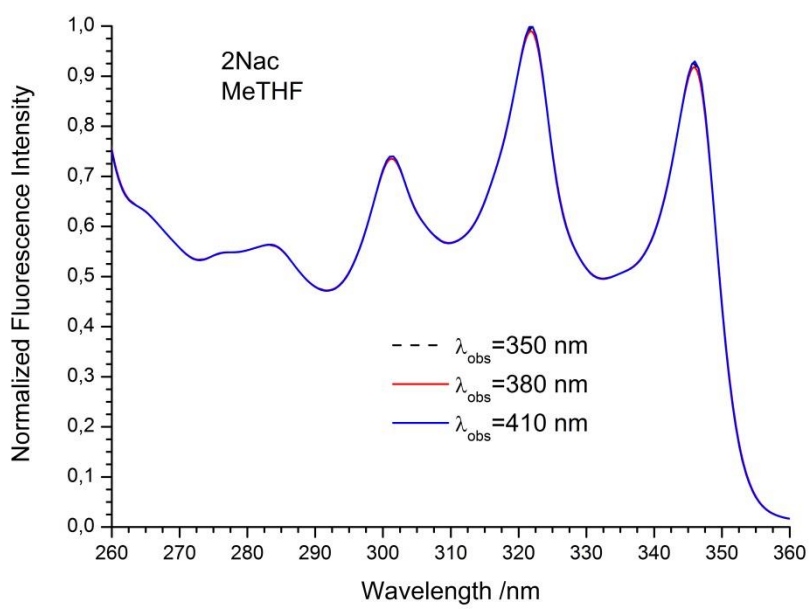


Fig. 19 ESI Fluorescence excitation spectra of 2Nac in 2-methyltetrahydrofuran recorded at different observation wavelengths.

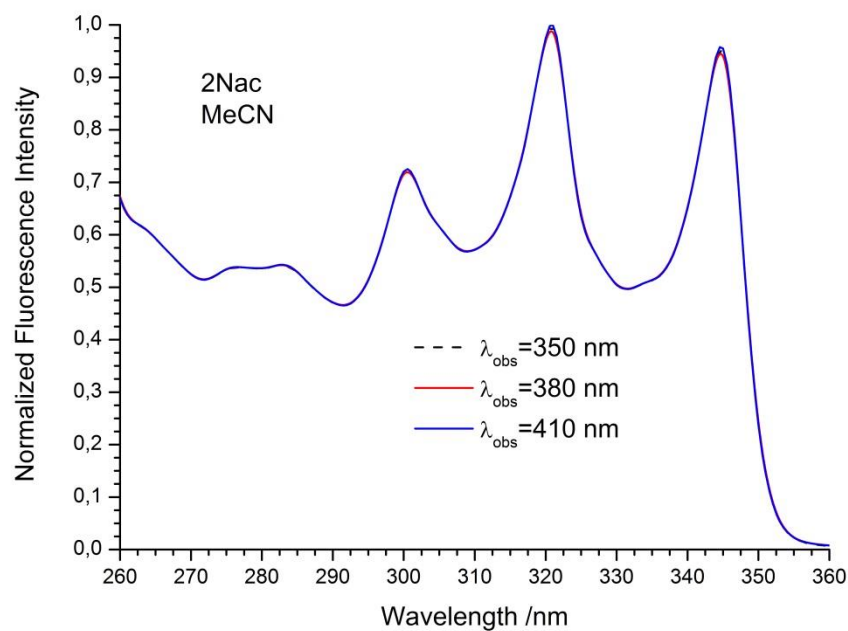


Fig. 20 ESI Fluorescence excitation spectra of 2Nac in acetonitrile recorded at different observation wavelengths.

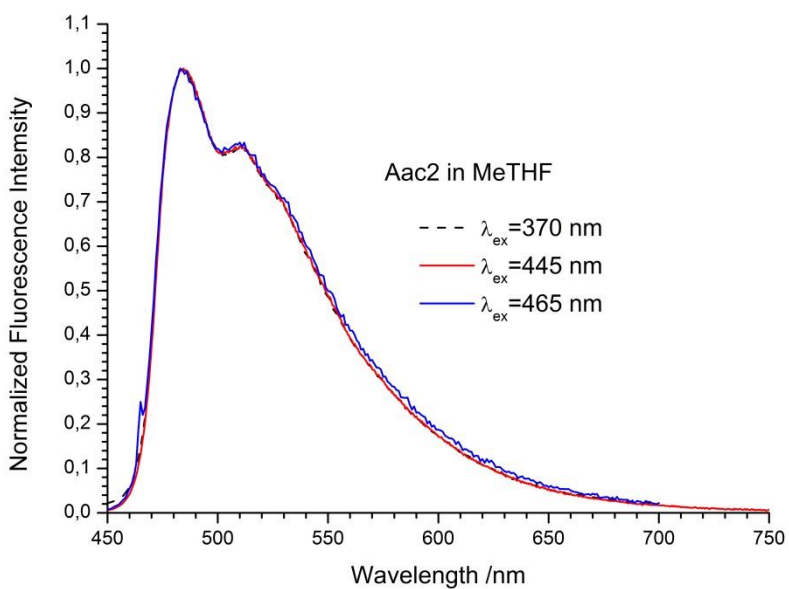


Fig. 21 ESI Emission spectra of Aac2 in 2-methyltetrahydrofuran recorded at different excitation wavelengths.

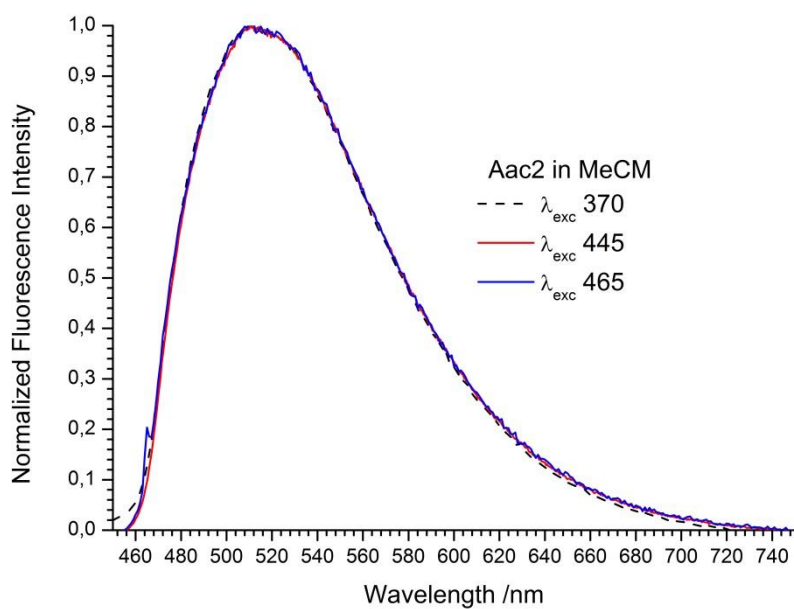


Fig. 22 ESI Emission spectra of Aac2 in acetonitrile recorded at different excitation wavelengths.

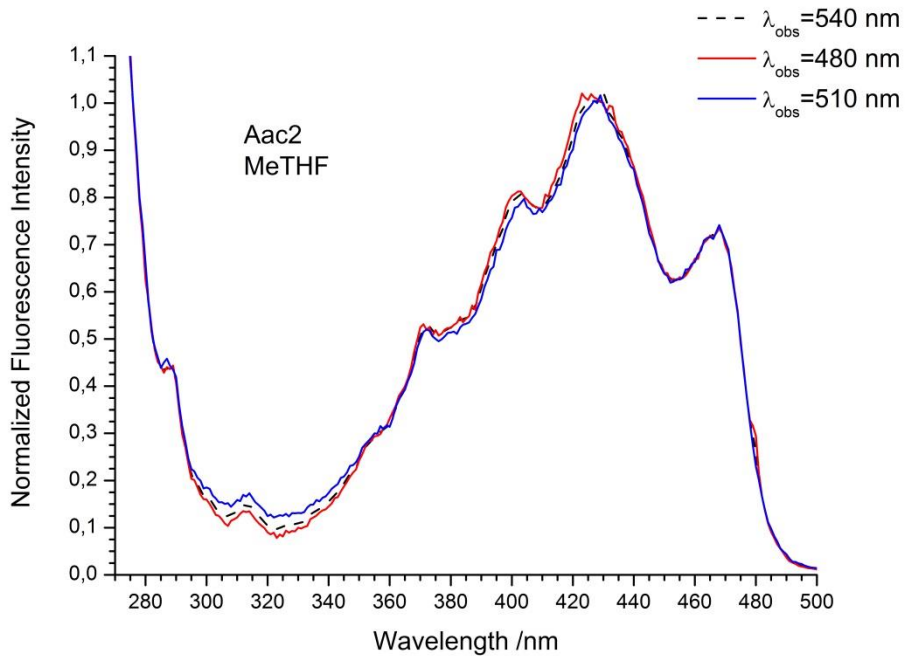


Fig. 23 ESI Fluorescence excitation spectra of Aac2 in 2-methyltetrahydrofuran recorded at different observation wavelenghts.

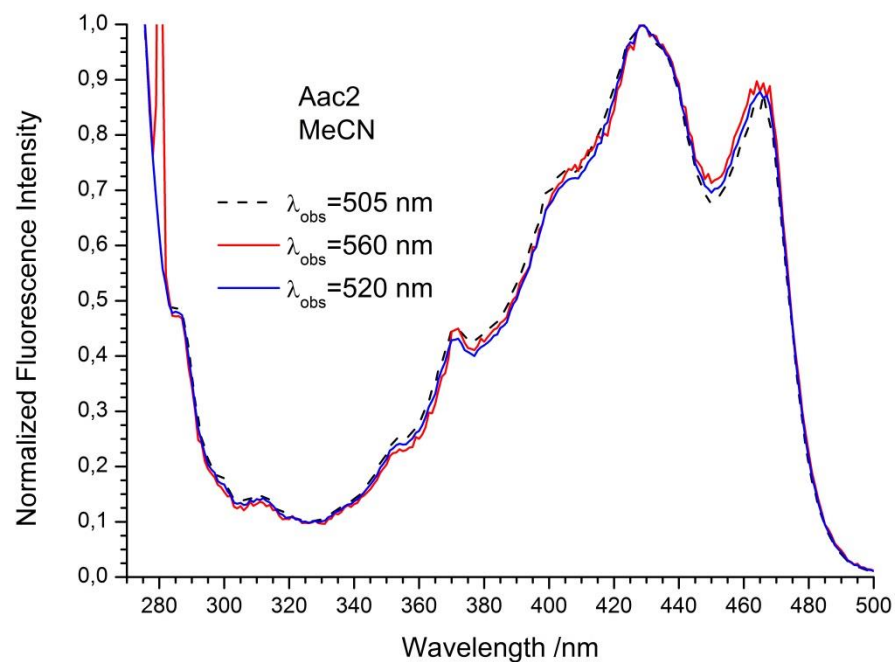


Fig. 24 ESI Fluorescence excitation spectra of Aac2 in acetonitrile recorded at different observation wavelenghts.

Table 3 ESI Fluorescence quantum yields of naphthyl derivatives of acetylene and buta-1,3-diyne recorded for different excitation wavelengths.

Compound	Solvent	$\phi (\lambda_{exc})$
1Nac	MeCN	0,7452 (340 nm) 0,7203 (360 nm)
	MeTHF	0,8510 (340 nm)
	MCH	0,8300 (360 nm) 0,7361 (340 nm)
		0,7202 (360 nm)
1Nac ₂	MeCN	0,0916 (330 nm) 0,0934 (345 nm)
	MeTHF	0,1651 (330 nm) 0,1634 (345 nm)
	MCH	0,1604 (330 nm) 0,1643 (345 nm)
2Nac	MeCN	0,1087 (320 nm) 0,0948 (310 nm) 0,1001 (330 nm)
	MeTHF	0,1189 (320 nm) 0,1099 (310 nm) 0,1131 (330 nm)
	MCH	0,1099 (320 nm) 0,1003 (310 nm) 0,1073 (330 nm)
2Nac2	MeCN	0,0034 (330 nm) 0,0037 (310 nm)
	MeTHF	0,0061 (330 nm) 0,0058 (310 nm)
	MCH	0,0100 (330 nm) 0,0096 (310 nm)

Table 4 ESI The radiative and non-radiative rate constant of acetylene and buta-1,3-diyne derivatives in polar (MeCN), low-polar (2-MeTHF) and non-polar (MCH) solvents.

compound	solvent	$k_r * 10^{-8} / s^{-1}$	$k_{nr} * 10^{-8} / s^{-1}$
1Nac	MeCN	4.09	1.40
	2-MeTHF	5.39	1.02
	MCH	4.95	0.97
1Nac2	MeCN	3.46	38.2
	2-MeTHF	6.11	30.9
	MCH	5.51	29.0
Pac	MeCN	4.77	0.42
	2-MeTHF	6.40	0.09
	MCH	7.11	0.18
Pac2	MeCN	4.52	1.73
	2-MeTHF	5.83	1.86
	MCH	6.83	1.96
Aac	MeCN	3.65	1.73
	2-MeTHF	3.78	1.94
	MCH	3.66	2.11

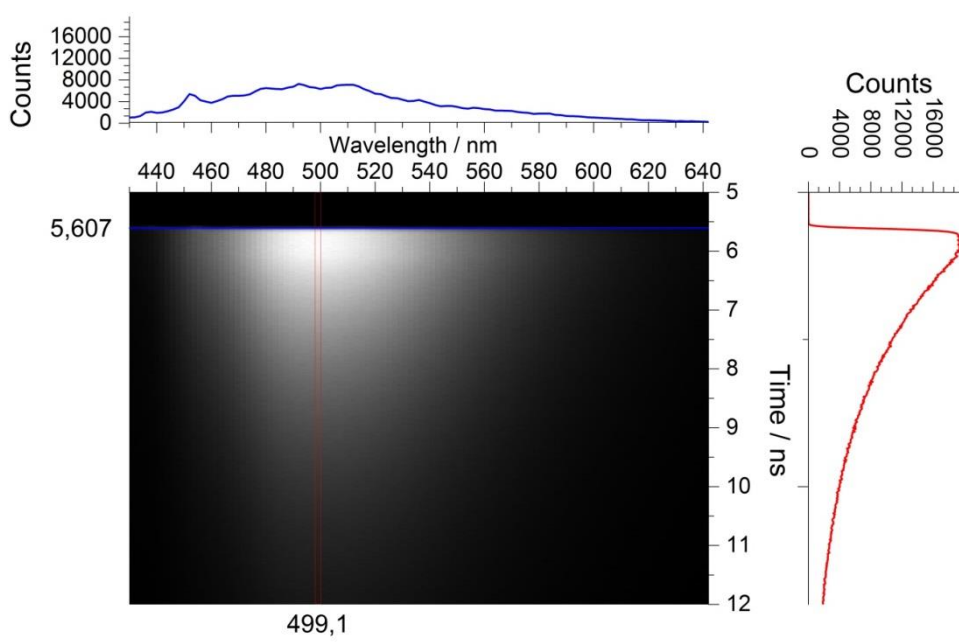


Fig. 25 ESI Time-resolved fluorescence image of Aac in acetonitrile as well as time – resolved emission spectrum and its fluorescence intensity decay extracted from the image.

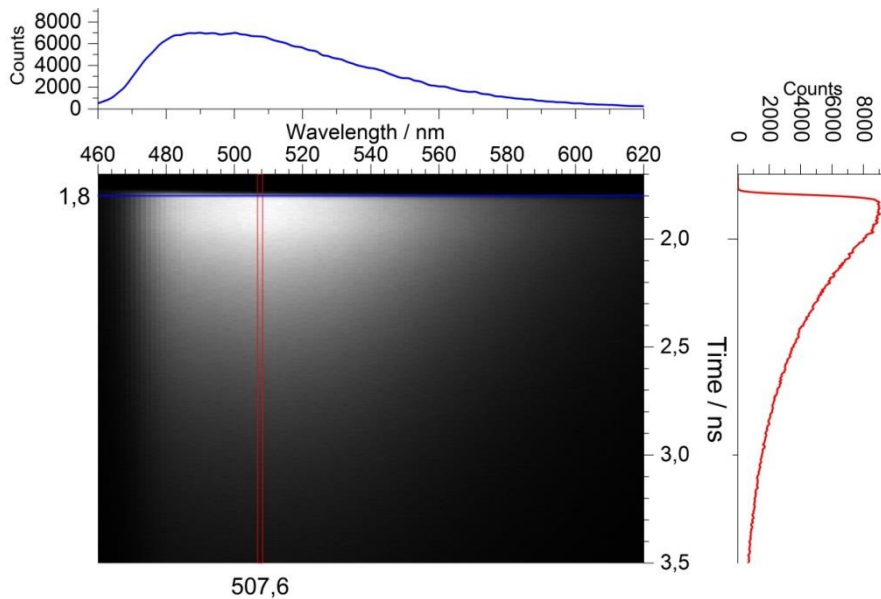


Fig. 26 ESI Time-resolved fluorescence image of Aac₂ in acetonitrile as well as time – resolved emission spectrum and its fluorescence intensity decay extracted from the image.

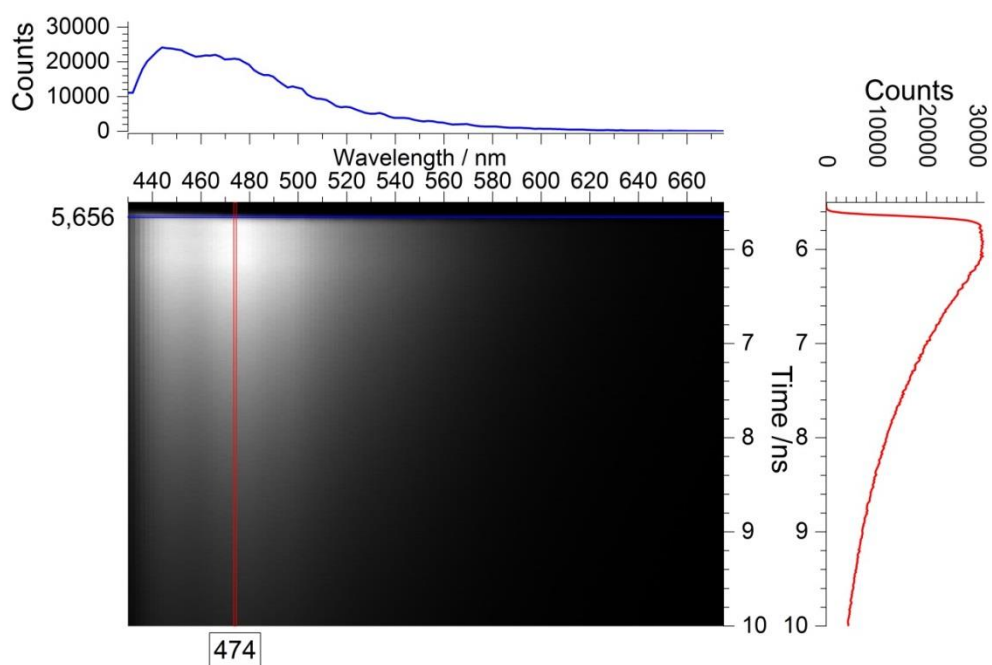


Fig. 27 ESI Time-resolved fluorescence image of Pac in acetonitrile as well as time – resolved emission spectrum and its fluorescence intensity decay extracted from the image.

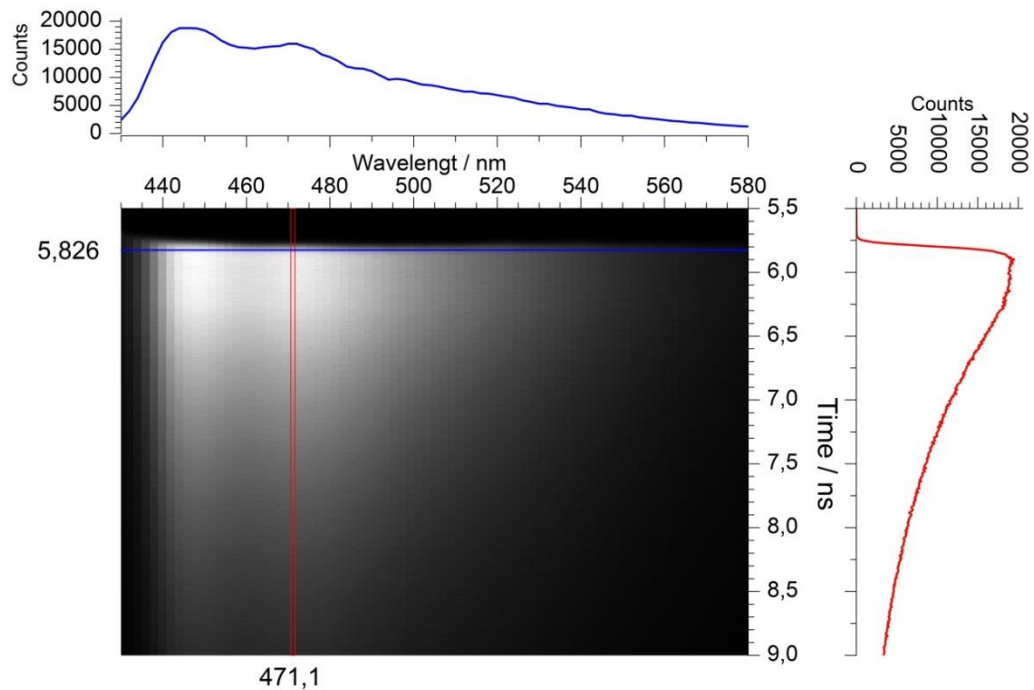


Fig. 28 ESI Time-resolved fluorescence image of Pac2 in acetonitrile as well as time – resolved emission spectrum and its fluorescence intensity decay extracted from the image.

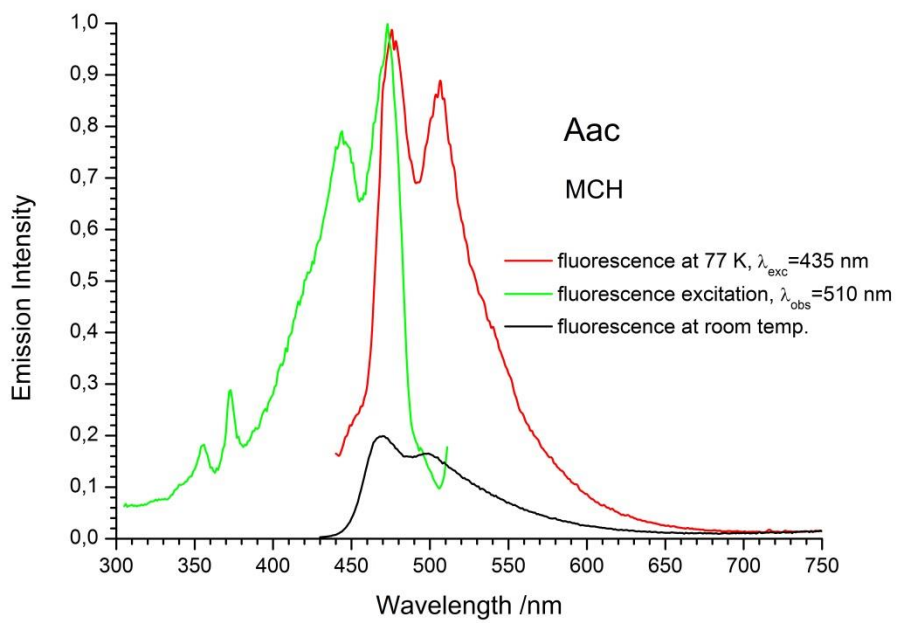


Fig 29 ESI The normalized emission (solid red line), and excitation (solid green line) spectrum measured at 77 K and fluorescence spectrum measured at room temperature (black solid line) of Aac in methylcyclohexane.

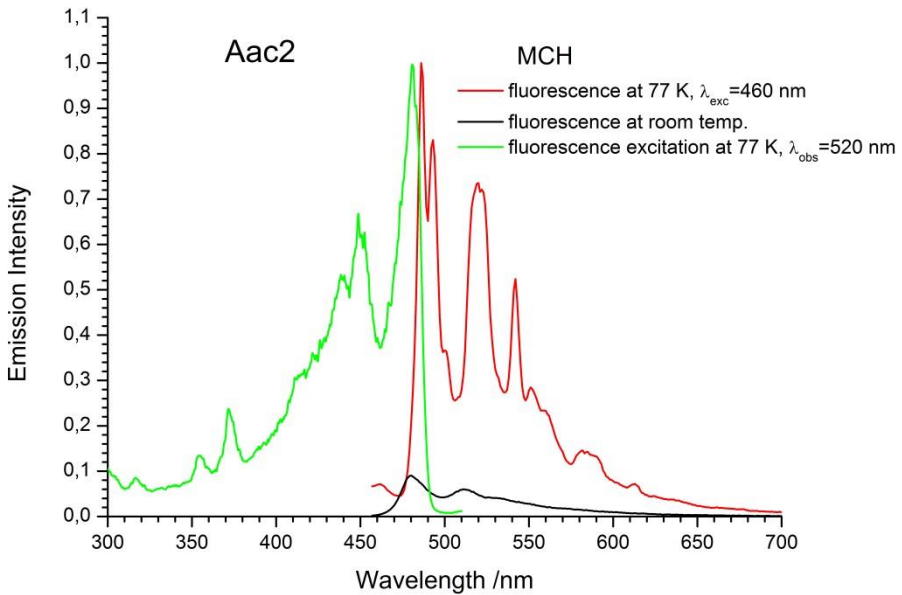


Fig 30 ESI The normalized emission (solid red line), and excitation (solid green line) spectrum measured at 77 K and fluorescence spectrum measured at room temperature (black solid line) of Aac2 in methylcyclohexane.

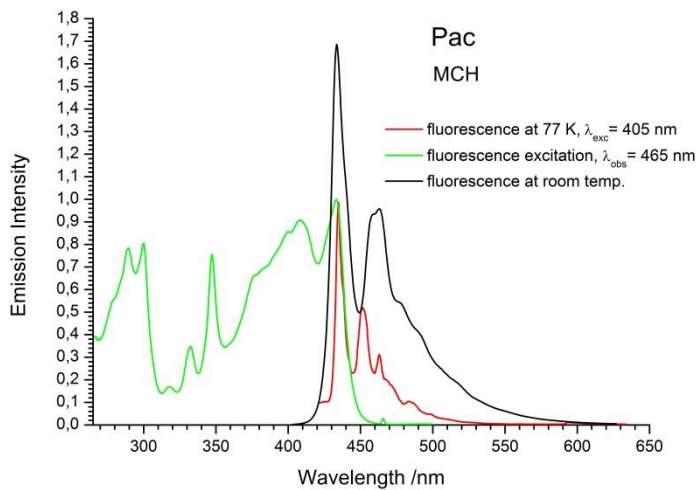


Fig 31 ESI The normalized emission (solid red line), and excitation (solid green line) spectrum measured at 77 K and fluorescence spectrum measured at room temperature (black solid line) of Pac in methylcyclohexane.

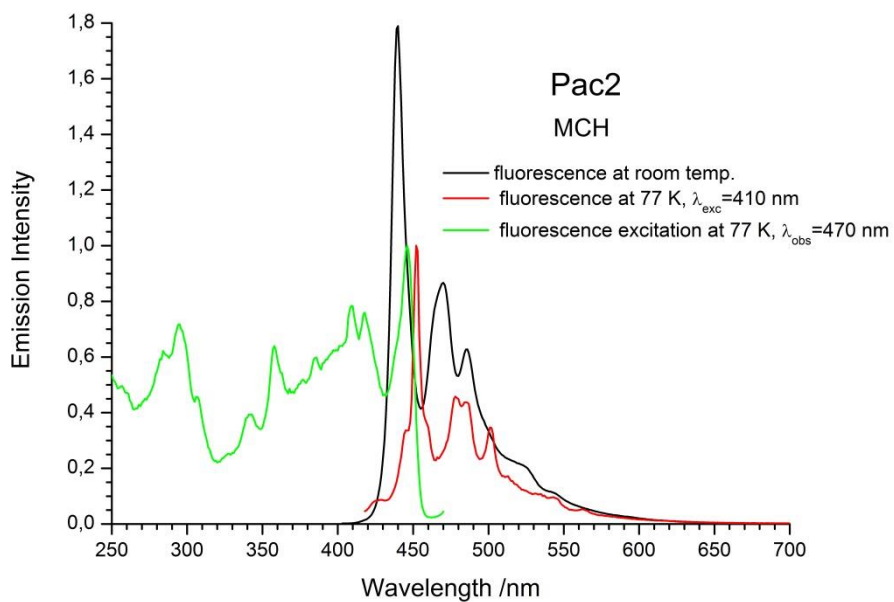


Fig 32 ESI The normalized emission (solid red line), and excitation (solid green line) spectrum measured at 77 K and fluorescence spectrum measured at room temperature (black solid line) of Pac2 in methylcyclohexane.

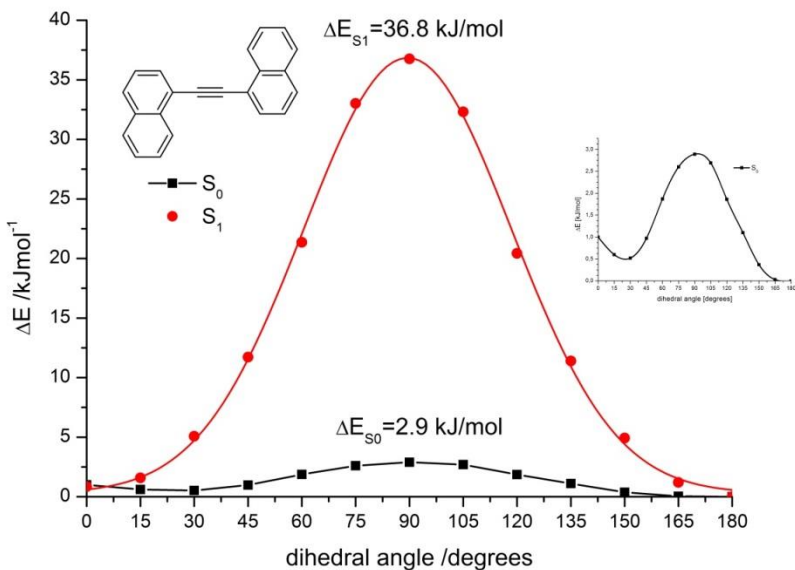


Fig. 33 ESI Potential of rotation energy of $\text{C}_{\text{Ph}}-\text{C}\equiv\text{C}$ bond of 1Nac in the ground state (black solid line) and excited state (red solid line). Insert show the enlarged potential of rotation energy in the ground state.

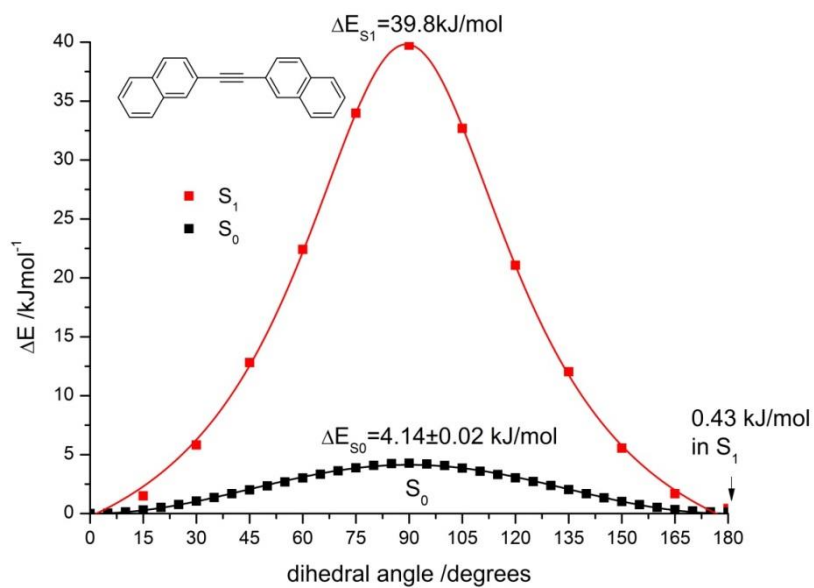


Fig. 34 ESI Potential of rotation energy of $\text{C}_{\text{Ph}}-\text{C}\equiv\text{C}$ bond of 2Nac the ground state (black solid line) and excited state (red solid line).

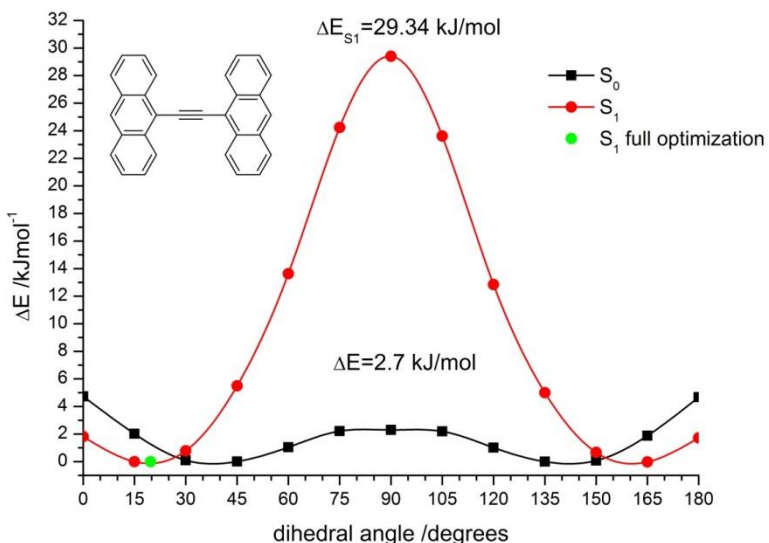


Fig 35 ESI Potential of rotation energy of $\text{C}_{\text{Ph}}-\text{C}\equiv\text{C}$ bond of Aac in the ground state (black solid line) and excited state (red solid line). The green point show the excited state energy for fully optimized Aac structure.

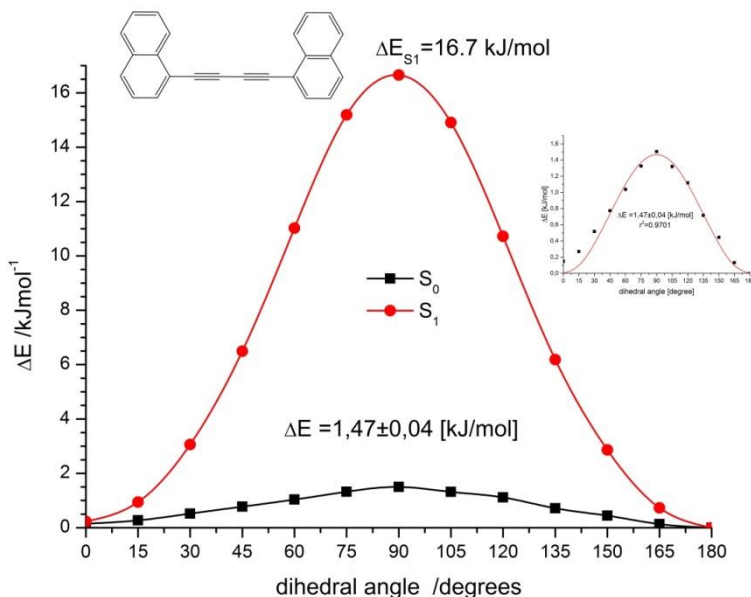


Fig 36 ESI Potential of rotation energy of $\text{C}_{\text{Ph}}-\text{C}\equiv\text{C}$ bond of 1Nac2 in the ground state (black solid line) and excited state (red solid line). Insert show the enlarged potential of rotation energy in the ground state.

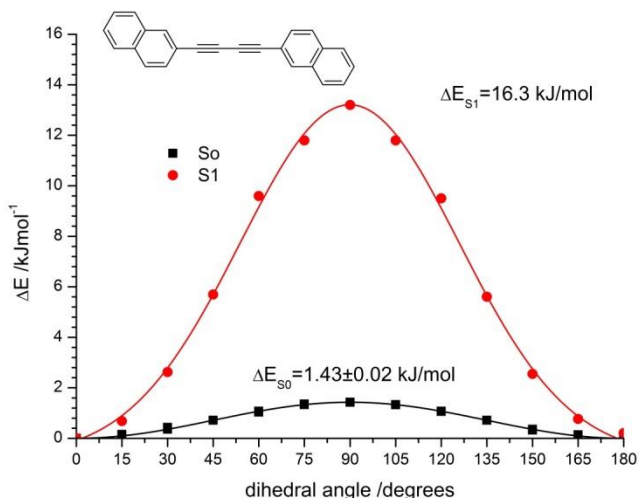


Fig 37 ESI Potential of rotation energy of $\text{C}_{\text{Ph}}-\text{C}\equiv\text{C}$ bond 2Nac2 in the ground state (black solid line) and excited state (red solid line).

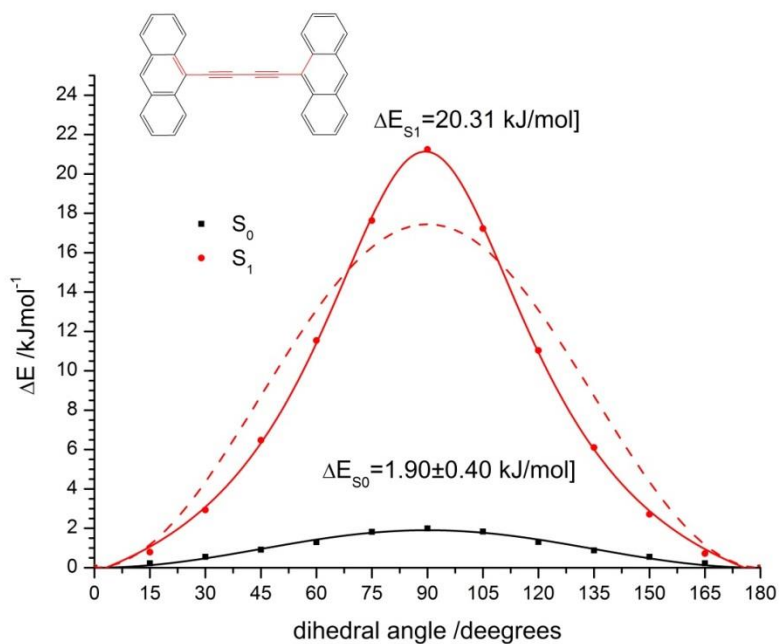


Fig 38 ESI Potential of rotation energy of $\text{C}_{\text{Ph}}-\text{C}\equiv\text{C}$ bond of Aac2 in the ground state (red dashed line) and excited state (red solid line). Dashed lines are the best fit to the equation $V/2(1-\cos 2\theta)$, whereas the red solid line to the Gauss function and green dotted line to Lorentz function.

Table 5 ESI The energy barrier of rotation (ΔE) of aryl acetylene and buta-1,3-diyne derivatives in the ground (S_0) and excited state (S_1) and rate constant of barrier crossing (k) and rotamer lifetime (τ).

derivative	$\Delta E (S_0)$ / kJmol $^{-1}$	$k \cdot 10^{-12}$ / s $^{-1}$	τ / fs	$\Delta E (S_1)$ / kJmol $^{-1}$	$k \cdot 10^{-7}$ / s $^{-1}$	τ / ns
1Nac	2.9	2.12	47	36.8	0.26	379
2Nac	4.1	1.31	76	39.8	0.079	1261
Aac	2.7	2.30	43	29.3	5.35	18.7
1Nac2	1.5	3.72	27	16.7	836	0.12
2Nac2	1.4	3.88	26	16.3	984	0.10
Aac2	1.9	3.17	32	21.3	132	0.76

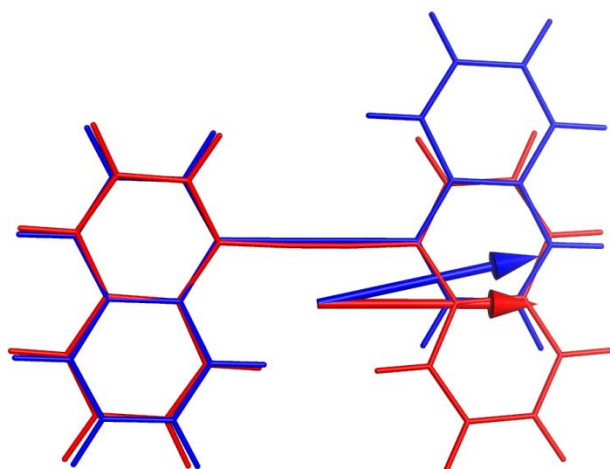


Fig. 39 ESI Fully optimized structures of cis (red) and trans (blue) rotamers of 1Nac in the ground state and transition dipole moments of the longest wavelength vertical transition in absorption.

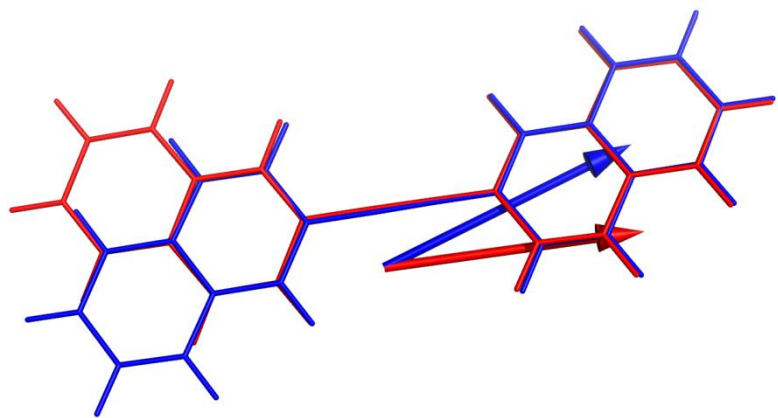


Fig. 40 ESI Fully optimized structures of cis (red) and trans (blue) rotamers of 2Nac in the ground state and transition dipole moments of the longest wavelength vertical transition in absorption.

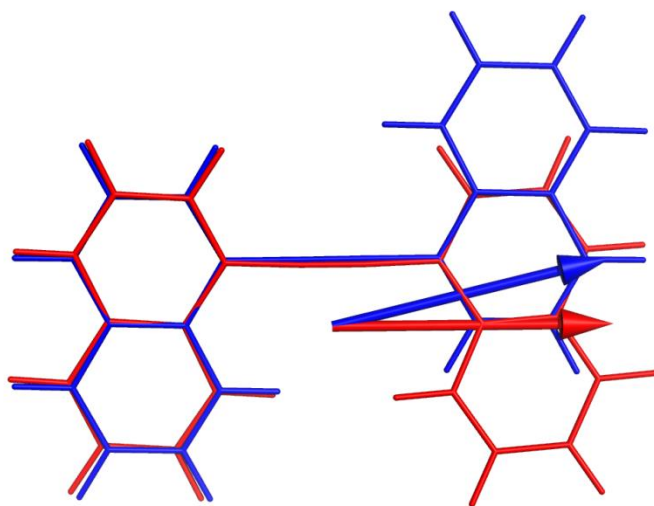


Fig. 41 ESI Fully optimized structures of cis (red) and trans (blue) rotamers of 1Nac in the excited state and transition dipole moments of vertical transition in emission.

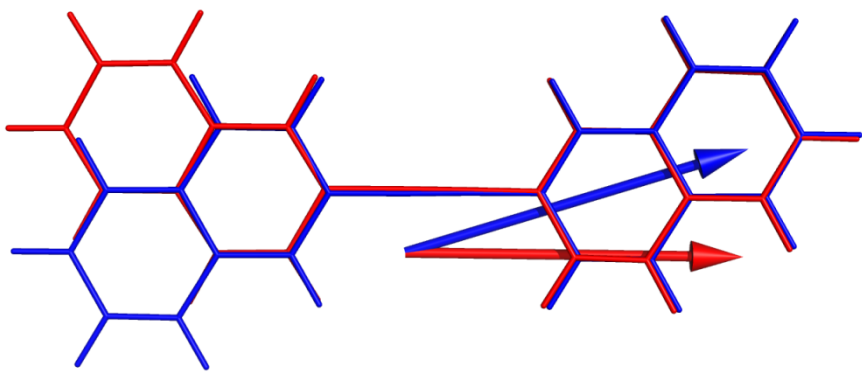


Fig. 42 ESI Fully optimized structures of cis (red) and trans (blue) rotamers of 2Nac in the excited state and transition dipole moments of vertical transition in emission